A&A 411, L131–L139 (2003)
DOI: 10.1051/0004-6361:20031224

Astronomy & Astrophysics

IBIS: The Imager on-board INTEGRAL

P. Ubertini[1], F. Lebrun[2], G. Di Cocco[3], A. Bazzano[1], A. J. Bird[4], K. Broenstad[5], A. Goldwurm[2], G. La Rosa[6], C. Labanti[3], P. Laurent[2], I. F. Mirabel[2], E. M. Quadrini[7], B. Ramsey[8], V. Reglero[9], L. Sabau[10], B. Sacco[6], R. Staubert[11], L. Vigroux[2], M. C. Weisskopf[8], and A. A. Zdziarski[12]

[1] Istituto di Astrofisica Spaziale e Fisica Cosmica, CNR, via del Fosso del Cavaliere 100, 00133 Roma, Italy
[2] CEN, Saclay, 91191 Gif-sur-Yvette Cedex, France
[3] IASF-Bologna, via P. Gobetti 101, 40129 Bologna, Italy
[4] School of Physics and Astronomy, University of Southampton, Highfield, Southampton, S017 1BJ, UK
[5] University of Bergen, Allegaten 55, 5007 Bergen, Norway
[6] IASF-Palermo, via U. La Malfa 153, 90146, Palermo, Italy
[7] IASF-Milano, via Bassini 15, 21033, Milano, Italy
[8] Marshall Space Flight Center, NASA, Ec 43, 35812 Huntsville, Alabama, USA
[9] University of Valencia, Dr. Moliner 50, 46100 Burjasot, Spain
[10] INTA, Carretera de Ajalvir km. 4 Torrejon 28691, Torrejon de Arzon (Madrid), Spain
[11] Univ. of Tübingen, Inst. for Astronomy and Astrophysics (IAAT), Sand 1, 72076 Tübingen, Germany
[12] Copernicus Astronomical Centre Bartycka 18 00716 Warsaw, Poland

Received 9 July 2003 / Accepted 8 August 2003

Abstract. The IBIS telescope is the high angular resolution gamma-ray imager on-board the INTEGRAL Observatory, successfully launched from Baikonur (Kazakhstan) the 17th of October 2002. This medium size ESA project, planned for a 2 year mission with possible extension to 5, is devoted to the observation of the gamma-ray sky in the energy range from 3 keV to 10 MeV (Winkler 2001). The IBIS imaging system is based on two independent solid state detector arrays optimised for low (15−1000 keV) and high (0.175−10.0 MeV) energies surrounded by an active VETO System. This high efficiency shield is essential to minimise the background induced by high energy particles in the highly excentric out of van Allen belt orbit. A Tungsten Coded Aperture Mask, 16 mm thick and ∼1 squared meter in dimension is the imaging device. The IBIS telescope will serve the scientific community at large providing a unique combination of unprecedented high energy wide field imaging capability coupled with broad band spectroscopy and high resolution timing over the energy range from X to gamma rays. To date the IBIS telescope is working nominally in orbit since more than 9 month.

Key words. INTEGRAL – IBIS – gamma-ray imaging

1. Introduction

After the Proton and the S/C engines had properly injected Integral in the final orbit the S/C and the Payload become fully operational. Then IBIS was switched-on and a short Performance Verification (PV) started, followed by an accurate Calibration phase. Main astrophysical target for the instrument tuning were Cyg X-1 region, to check the imaging capability and the Point Source Location Accuracy (PSLA), two different high latitude Empty Fields, for background evaluation and flat fielding purpose, and a short Galactic Plane Scan, to check the IBIS short integration time observation (∼2000 s) sensitivity in the soft γ-Ray range (15−200 keV).

The PV phase result has basically confirmed the anticipated IBIS Scientific Performance, i.e. a fine angular resolution of ∼12 arcmin, PSLA of 1−2 arcmin, wide spectral response (15 keV to 10 MeV), high time resolution (61 μs), spectroscopy (9% at 100 keV and 10% at 1 MeV), required to satisfy the mission's imaging and broad line spectroscopy objectives.

During the PV phase the first Integral Gamma Ray Burst GRB 251102) was detected in almost real time, from 15 keV, the lower energy range of the instrument, up to 500 keV. At that point the instrument was fully operative to perform observations on the 3 day based orbit transmitting scientific data via the real time telemetry link at the about 60 kbit/s allocated to IBIS. Since the beginning of 2003 Core Programme and Open Time scientific observations have successfully started. The scientific programme comprised regular scan of the Galactic Plane (GPS), Galactic Centre Deep Exposure (GCDE), Open Time standard pointing and associated ToO observations. In addition several new soft gamma ray sources have been discovered (Winkler et al. 2003) and six Gamma Ray Bursts detected

Send offprint requests to: P. Ubertini,
e-mail: ubertini@rm.iasf.cnr.it

Fig. 1. The IBIS Detector Unit during final mechanical integration on the S/C at ESTEC: in the picture are visible the Veto BGO modules, the Hopper structure and the Payload Module with the open Detector housing; the internal black wall is part of the Lead Passive Shield extending up to the Coded Mask.

within the IBIS coded FoV (Ubertini 2003) confirming the anticipated rate of ∼1 GRB/month. In Table 1 is shown a summary of the IBIS scientific performance. In Fig. 1 is shown the IBIS Detector Module during insertion into the INTEGRAL Payload Module, shown in Fig. 2 with the Detector Module in place.

2. IBIS hardware configuration

2.1. ISGRI: The CdTe detector array layer

The low energy matrix (128×128) features a novel large area (∼2600 cm^2) multilayer CdTe detectors (Lebrun et al. 2003). The cadmium telluride is a II–VI semiconductor operating at ambient temperature. With their small area, the CdTe detectors are ideally suited to build up a pixellated imager with good spatial resolution. On the other hand, their small thickness restricts their use to the low energy domain (50% efficiency at 150 keV). Providing spectral performance intermediate between the cooled germanium spectrometers and the scintillators, the CdTe can be used way down in the X-ray domain ($E > 15$ keV). In Fig. 3 is shown one CdTe Module Detector Unit.

2.2. PICsIT: The CsI detector array layer

The high energy matrix (64×64) uses novel caesium iodide elements red out with photodiodes (Labanti et al. 2003) and features a sensitive area of 2890 cm^2. Caesium Iodide is a I–VII scintillation crystal. The CsI(Tl) bars are optically bonded to custom made low leakage silicon PIN photodiodes, designed for optimal performance at 511 keV. The design provides a high degree of modularity. The CsI layer is divided in eight rectangular modules of 512 detector elements, each module is integrated into a stand-alone testable sub-system. Modules may be assembled into the layer. The CsI modules have the same cross-sectional shape as those of the CdTe ones (Ubertini et al. 1999). In Fig. 4 is shown one CsI Module Detector Unit.

2.3. The Compton telescope function

The separation between the CsI crystals upper surfaces and the CdTe is about 94 mm. The double-layer-discrete-element design allows the paths of interacting photons to be tracked in 3D if the event triggers the two layers and not trigger the Veto system. In this way it is possible to apply the Compton kinematics reconstruction algorithms to this type of events. Taking into account the $\sigma_{\rm Comp}$ for the two detectors this interaction have the

Table 1. IBIS scientific facts.

Parameter	Value
Energy range	15 keV–10 MeV
Sensitive area	2600 cm^2 CdTe, 2890 cm^2 CsI
Energy resolution at 100 keV and at 1 MeV	9% and 10% (singles)
Field of view fully coded and partially coded	9° and 19° (50%)
Continuum sensitivity 3σ, 10^6 s, at 100 keV and 1 MeV (ph cm^{-2} s^{-1} keV^{-1})	3.8×10^{-7} and 5.0×10^{-7}
Line sensitivity 3σ, 10^6 s, at 100 keV and 1 MeV (ph cm^{-2} s^{-1})	1.3×10^{-5} and 3.8×10^{-4}
Angular resolution	12 arcmin
Point source location accuracy	30 arcsec
Timing resolution	61 μs (for $E < 1$ MeV and Compton), 1 ms (Spectral timing, no imaging) 2000 s ($E \geq 175$ keV with imaging)

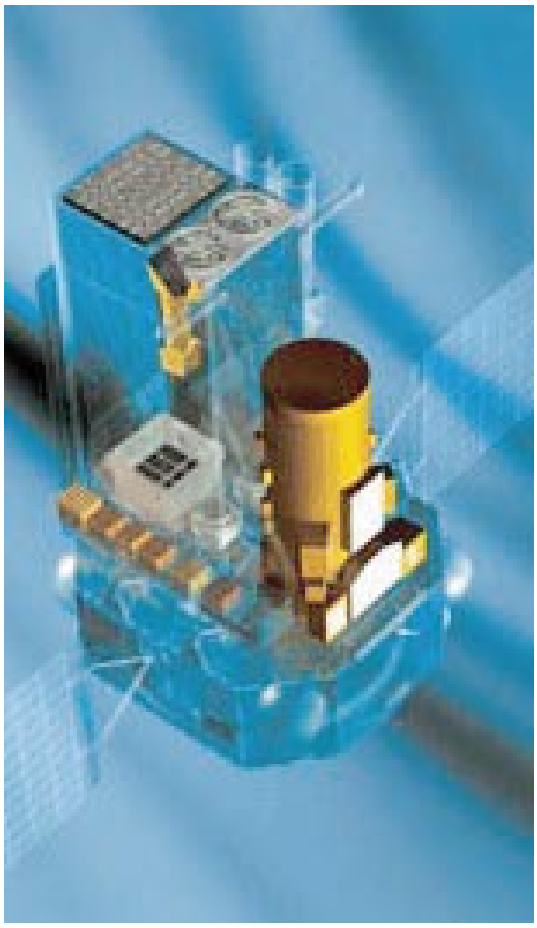

Fig. 2. The Integral Payload Module view in the direction of IBIS: as shown in the drawing the field of view of the detector array is confined by a 1.0 mm thick Tungsten Hopper (grey) 550 mm high. Then the detector aperture is further restricted by a Tube made out of a graded thin lead passive shield (light blue) embedding the space between the mask and the top part of the Hopper. Finally the side part of the Coded Mask is shielded by 1.5 mm lead strips. This shield set up is almost completely opaque to the soft gamma-ray diffuse radiation preventing any photon leaks in the energy range below 200 keV.

maximum probability to occur between few hundred keV and few MeV, and allows an increase in signal to noise ratio attainable by rejecting those events likely to correspond to source photons outside the FOV.

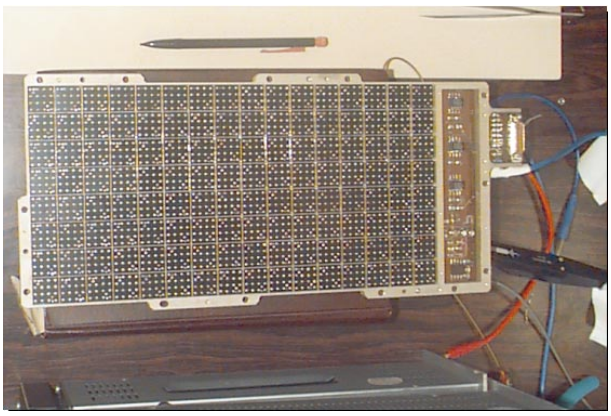

Fig. 3. One of the ISGRI Molules during Test.

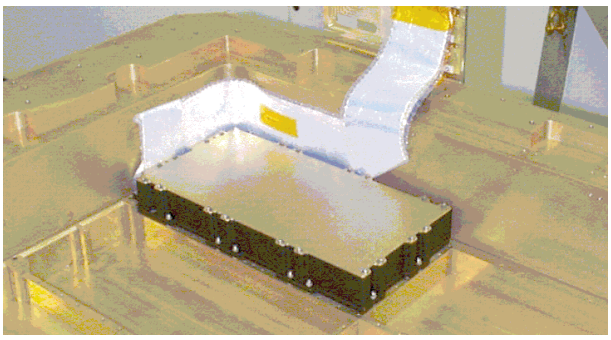

Fig. 4. One of the PICsIT Modules during pre-assembly.

2.4. Active anticoincidence system

The Veto system is a five side "cage", completely embedding the high energy detector and extending just up the low energy array. The anticoincidence system is composed by 16 independent modules, the Veto Detector Modules (VDM), each made out with 2 large BGO crystals ~150×75 mm^2, 20 mm thick each, optically coupled together (see Fig. 5), read out by two 3 inches Photomultipliers. Each Veto Detector Module includes: the two BGO crystal and related housing, two PMT's optically coupled to the BGO and assembled with the dedicated FEE and HV divider, one HV Power Supply and one Veto Module Electronics for Module control (Quadrini et al. 2003). The Veto system is arranged in two halves: 8 lateral

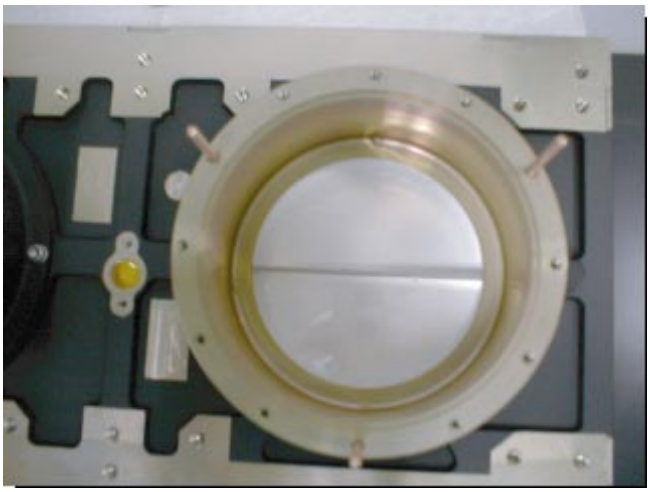

Fig. 5. View of one VDM during assembly: the optical join between the two BGO slabs is visible through the quartz window housing the 3 inch Photomultiplier.

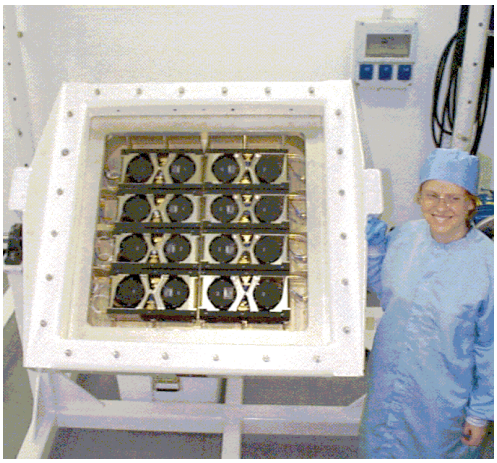

Fig. 6. The 8 VDM modules of the "bottom" array are visible.

VDM shields, i.e. 2 per detector side, and 8 bottom VDM modules completely covering the bottom part of the detector (see Fig. 6). This set up ensure very limited "leaks" to environmentally produced photons and cosmic/solar charged particles and it is not very sensitive to pile up induced by large energy (and in turn light) release due to high energy protons or heavy ions detected by the BGO assembly. In this way the thick BGO crystals ensure a substantial photon absorption up to ~2 MeV and an outstanding active shielding with a threshold ≤80 keV. The VDM provide a moderate spectral resolution, allowing a daily calibration of the BGO gain and threshold with the use of the 511 and 1275 keV tagged lines from the on board calibration unit. So far no drift in the HV nor of the thresholds have been measured, confirming the rejection efficiency of the Veto system is quite stable. The long term trend of the Veto count rate is currently under study.

2.5. Collimating system and passive shields

The passive collimating system of IBIS is made of two subsystems mechanically independent based on tungsten and lead as

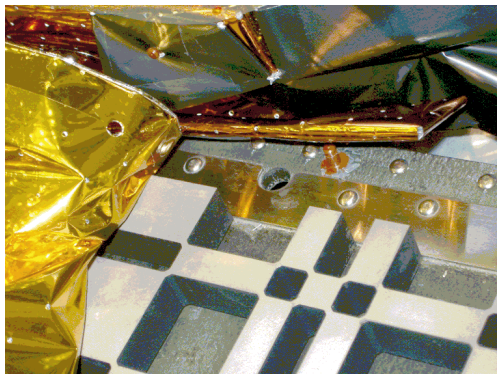

Fig. 7. Details of the Coded Mask: the joint between "pixels" and shielding strips are visible.

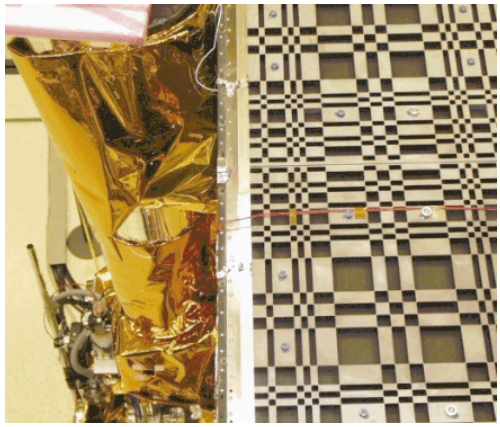

Fig. 8. the Mask in the direction of the star trackers. One of the star tracker baffle (left), covered with MLI is also visible.

passive material: (a) the "Hopper" a 550 mm height structure placed on the ISGRI layer and (b) a "Tube" made of four walls with a profile that ideally join the Hopper top part to the mask sides geometrically defining detector layers field of view. For the tube the adopted passive material is lead with a variable thickness distribution for mass minimisation while the hopper shielding is made of 1.0 mm thick tungsten layers. The passive shielding is designed to reduce the celestial diffuse background component as much as possible it is opaque up to about 200 keV.

2.6. The coded mask

The coded mask assembly lays at 3400 mm above the detector bench. The support is a 80 mm thick sandwich plate composed by two Carbon Fibre skins and a "Nomex" core. The Densimet (95%W-5%Cu) Mask, divided in four plates formed by 16 mm thick pixels interconnected by 2 mm ribs, is placed on the top part of the CFRP plate (see Figs. 7 and 8).

The coded mask projects a shadowgram onto the detector plane and images of the sky will be reconstructed by decoding the detector shadowgram with the mask pattern.

Half of the cells are opaque to photons in the operational energy range of the IBIS instrument, ensuring a minimum opacity of ~70% opacity at 3 MeV. The other 50% of cells are

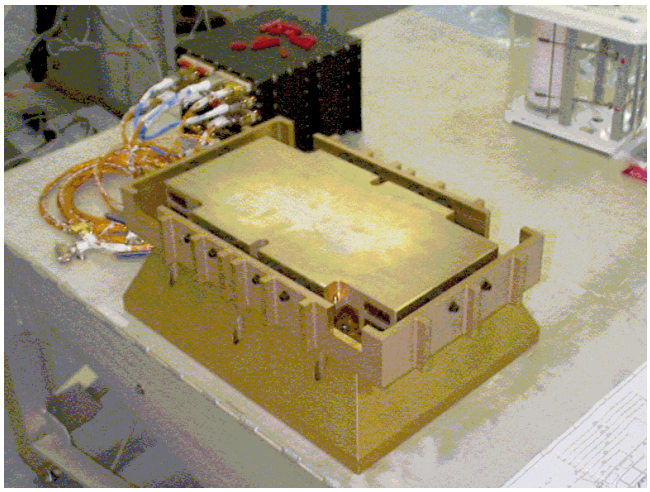

Fig. 9. The flight unit of the On board Calibration Unit during testing phase.

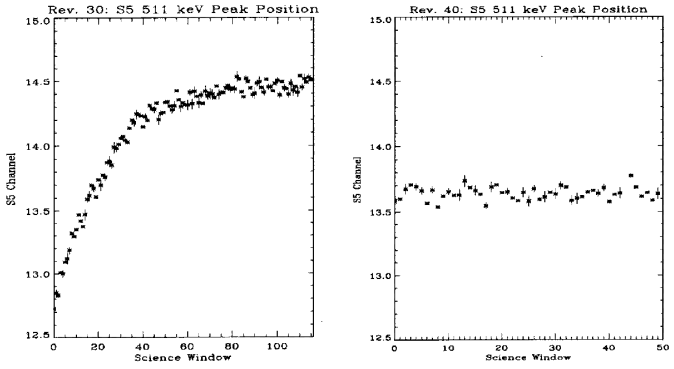

Fig. 10. PICsIT gain variation vs. time in two different orbits.

"open", i.e. with an off-axis transparency ranging from 60% at 20 keV up to about 95% at high energy. The Mask was aligned on ground by using two optical cubes with cross on the $+Y$ and $+Z$ mask reference axis. During flight operations the alignment is guaranteed by the structure of the PLM, which provides high rigidity and low thermal distortion in order to be able to achieve the 30 arcsec point source location accuracy, required by the scientific goal of IBIS.

2.7. On board calibration unit

On-board calibrations are necessary in order to monitor and control the instrument in flight performances and to reach the limit sensitivity on weak astronomical sources to be studied. The response function of the instrument is refined through comparison of predicted performances obtained by modelling and ground calibration with in-orbit measurements. The IBIS on board Calibration Unit (CU) will consist of 0.4 μ Ci ^{22}Na radioactive source placed near to the centre of the largest face of a BGO Detector Module (see Fig. 9). A tagging system is implemented in order to detect one of the two 511 keV photons emitted during the ^{22}Na decays and additionally can detect the 1275 keV photon which is emitted toward the tagging detector in 50% of the cases. The energy acceptance window is 100−2000 keV. In this way the gain and the thresholds of the high energy detector is calibrated to better than 1% accuracy in one revolution @511 keV and five revolutions @1275 keV. Also the low energy detector, albeit at low efficiency, will make use of the tagged 511 keV line. The on-board calibration system also allows the correction of main systematic errors (Bird et al. 2003a).

As an example of the importance of the CU data the Fig. 10 shows the PICsIT gain variation during the initial orbits due to temperature drift, when two modules out of eight were maintained on during belt passage. The 511 keV peak position versus time is shown for a full orbit (3 days). The data have been obtained from tagged photons generated by the CU and transmitted in the S5 calibration packets. Similar data are continuously transmitted at 1275 keV. As can be seen the temperature of the PICsIT layer was basically constant after half orbit i.e. ~30 hours. On the right panel same data set collected during a later orbit when all the eight modules were maintained on during belt passage. The temperature profile, and in turn the gain, is extremely constant being the gain variation less than 0.2% (Malaguti et al. 2003).

2.8. Data Handling System

The Data Handling System (DHS) is based on the Data Processing Electronics (DPE) and Hardware Event Preprocessor for IBIS (HEPI) that is necessary to cope with the overall processing requirements due to the high detector event rates that would correspond to a throughput up to 300 kbit/s if directly transmitted to ground. The DPE box provides a two way communication interface between the detectors and the S/C. All scientific data and housekeeping from the two imaging detectors as well as from the veto and the calibration system are collected, handled and finally channelled to the On Board Data Handling (OBDH) system for telemetry generation. In the other direction the DPE distributes to the instrument telecommands and clock informations. The DPE provides the capability to run IBIS in the different Scientific, Diagnostic, Patch/Dump, Stand by etc. modes. Science data from the CdTe are selected by energy thresholds. Compton data are selected by angle computation. All CsI histogram data (spectral timing, CsI single, multiple, calibration and polarimetric histograms) are compressed. After processing all data are packetised in the TM format and handed over to the OBDH. The TM generation is controlled by the Instrument Application Software (IASW) autonomously.

3. Initial switch-on, performance verification phase, IBIS first light and calibration

Soon after IBIS Electronics was fully activated the detector systems were switched on one by one. After all subsystems were checked to be nominal the scientific parameters optimisation started to optimise the following parameters: VETO-ISGRI delay and width, VETO-PICSIT delay and width, ISGRI-PICSIT time synchronization, VETO and CU Threshold and Gain. The proper PV started immediately to test the scientific data

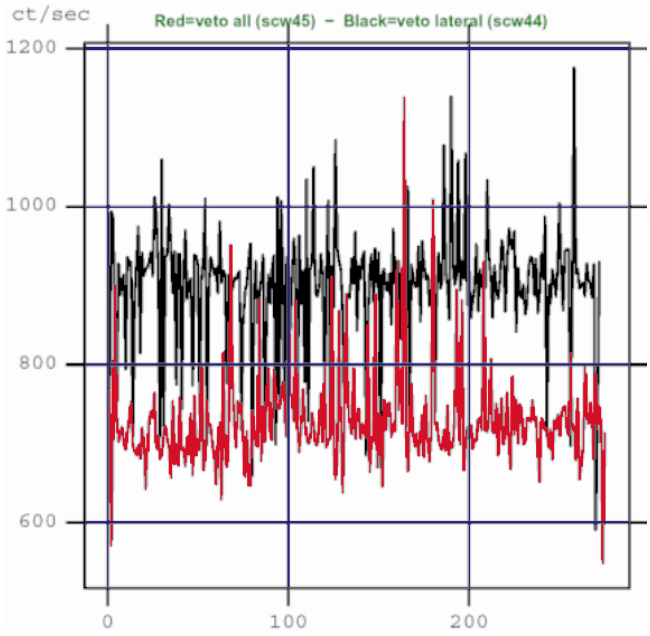

Fig. 11. The raw ct/s versus time, after on board Veto rejection applied before (black) and after (red) the SW patch to the Instrument Application Software.

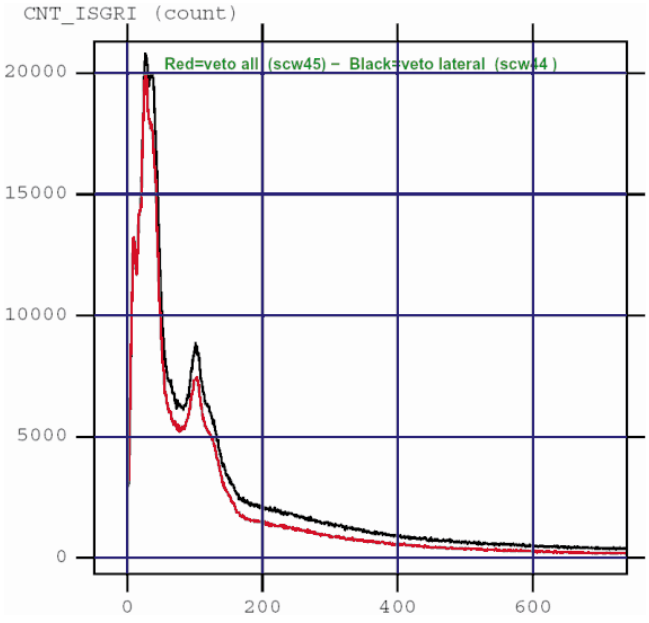

Fig. 12. The IBIS/ISGRI raw count spectrum: as can be seen the shape is not affected by the patch, being the "bad" triggers distribution monotonic over a large energy range.

mode: Photon-by-photon from ISGRI and PICsIT, Compton events, Calibration events from ISGRI and PICsIT with and without the CU tagging system, PICsIT spectral imaging histograms and Spectral Timing data, Science HK monitor, Veto and CU spectra etc. One of the long waited information was the Background counting rate, driving the IBIS sensitivity and the TLM occupation. It was confirmed that the in flight environment was strongly dominated by high energy protons and electrons and that the effect of the anticoincidence Veto System was working as anticipated (Quadrini et al. 2003). The background high energy values (PICsIT) was confirmed to be within the upper bound of the Montecarlo estimated ranges (Bird et al. 2003b; Di Cocco et al. 2003; Stephen et al. 2003). At lower energy (ISGRI) the BGD was very close to the predicted one, actually 10% worst, confirming the very good pre-launch estimation taking into account the so far unknown behaviour for CdTe detector in-flight (Lebrun et al. 2003). The presence of large pulses inducing non statistical counting rate in the PICsIT and ISGRI detector was noticed since the first activation. This effect resulted in very bright pixels multi-triggers generating linear and elliptical tracks in the detector images over time scale ranging from 0.1 ms to 0.1 s. This tracks were produced by delayed secondary triggers due to interaction of energetic cosmic rays with the detector (Hurley 1978; Segreto et al. 2003), and cannot be vetoed by the Anticoincidence. In principle, this tracks can be almost completely eliminated on ground after the data are transmitted in Ph/Ph mode. Unfortunately, this would have implied a substantial increase in the TLM rate to transmit the ISGRI scientific packets and a too high rate for PICsIT. The problem was deeply investigated and implies a slight degradation of the sensitivity of the high energy detector below 300 keV (Natalucci et al. 2003), when the scientific observation is carried out in the "Standard Science Mode". As far as the low energy detector it was possible to implement a "Patch" to the IASW on-board to discard the tracks on board. In the Fig. 11 and in the Fig. 12 is visible the drop in background counting rate, collected on an empty field, before (black) and after (red) the patch implementation, as well as the change of the background spectrum. In this way more than 250 meaningless ct/s are not transmitted to ground with a substantial TLM saving.

4. IBIS first light

IBIS was pointed toward the first strong celestial source i.e. the black hole candidade Cyg X-1 on November 16th 2002 (Bazzano et al. 2003). The real time data transmitted to ground were collected with Instrument ECOE at MOC/ESOC (Darmstadt). After a few minutes the mask shadowgram appeared projected onto the 128×128 CdTe detector array as shown in Fig. 13 confirming the unprecedented sensitivity and imaging capability of IBIS. Applying in almost real time a simple deconvolution algorithm to the data set the first IBIS/ISGRI astrophysical sky image appeared (15–50 keV) as shown in Fig. 14. Cyg X-1 and Cyg X-3 are visible in detector coordinate, integration time was 1800 s. In a similar way the IBIS/PICsIT "first light" of Cyg X-1 was obtained integrating over 29 ks exposure (190–300 keV) as shown in Fig. 15.

Finally, in Fig. 16 is shown the same IBIS/ISGRI field of the Cygnus region plotted in Sky coordinate. As can be seen the absolute positioning capability over a wide field of view is very good (Goldwurm et al. 2003). It turned out there was, after injection in orbit, a 10 arcmin misalignment between the star trackers and IBIS. The relevant correction was applied and since then the instrument is routinely positioning X and gamma ray sources with 2–3 arcmin radius accuracy.

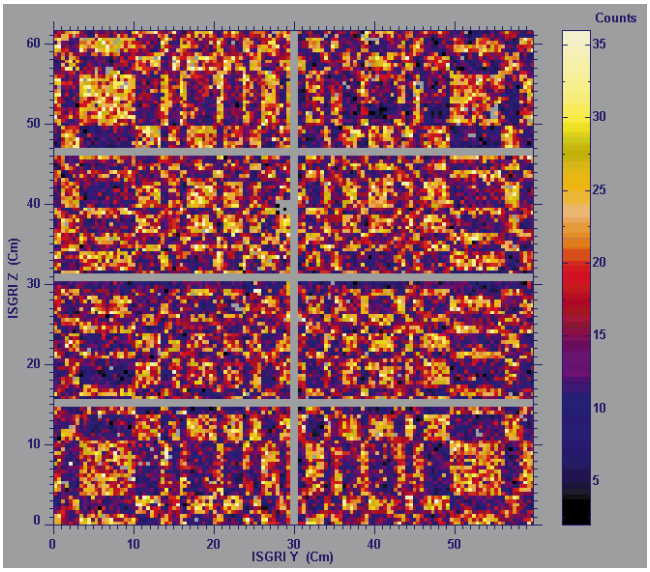

Fig. 13. IBIS/Integral First Light of the celestial source Cyg X-1: the mask shadow imprinted on the CdTe detector was clearly visible in almost real time after integrating over a few minutes.

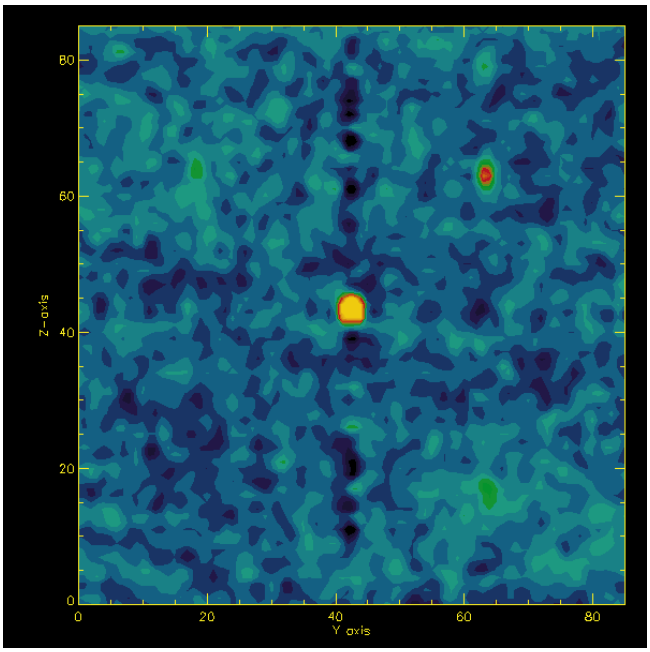

Fig. 14. IBIS/ISGRI first sky image (courtesy of L. Natalucci).

5. Calibration

As soon as the Crab was within the S/C permitted solar aspect an extensive calibration programme started and detailed reports are within this volume (cf. Malaguti et al. 2003; Terrier et al. 2003 and IBIS related papers). As a short exposure example in Fig. 17 is shown the IBIS/ISGRI Crab integrated count rate spectrum, as recorded during a staring observation lasting 10 ks. The three curves represent: magenta, background spectrum; blue On-Source spectrum (i.e., background plus Crab); yellow, Crab only. The data shown were collected in real time with the IBIS ground support equipment and demonstrate the

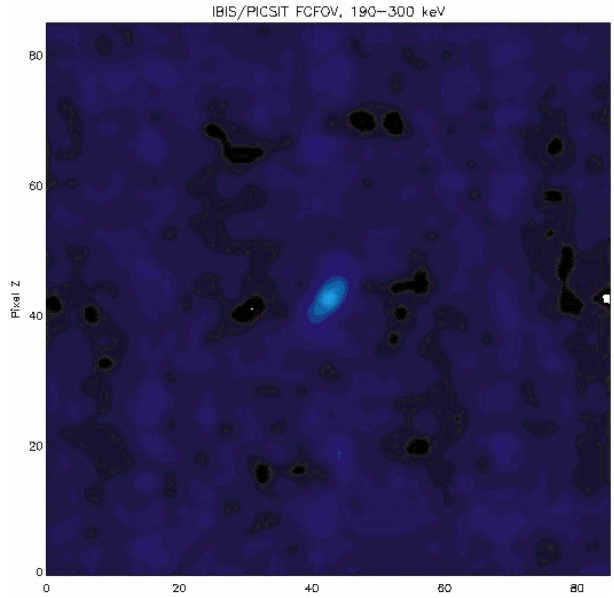

Fig. 15. The IBIS/PICsIT "first light" image of Cyg X-1, integrated over 29 ks, again in detector coordinate (Courtesy of L. Natalucci).

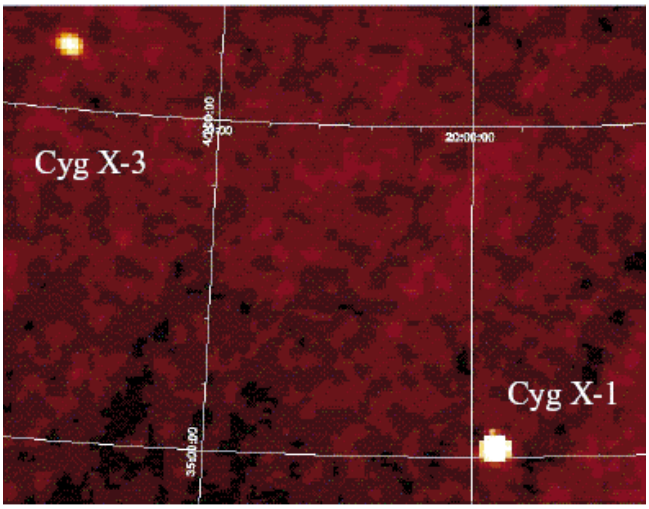

Fig. 16. The same data of Fig. 14 shown in Sky coordinate (15–50 keV).

capability to obtain a substantial signal from a Crab like source up to 150 keV in a short integration time.

In Fig. 18, is shown the Crab light curve at different energies as obtained in almost real during the initial IBIS Calibration. The Crab Pulsar double peak and the peak sharpness was an immediate confirmation of the good time capability of the instrument. The data are not barycentre corrected, the energy range of the different panels are 14–32.5, 32.5–55.0, 55.0–77.5 and 77.5–100.0 keV respectively (courtesy of A. Segreto, Calibration team). Finally, a beautiful example of the IBIS wide band coverage is shown in Fig. 19 the ISGRI and PICsIT detectors counting rate obtained during the strong GRB 251102. The data span from 15 keV up to about 500 keV and the region were the two detection layers overlap is clearly visible, corresponding to about 200 keV (Courtesy of A. Segreto).

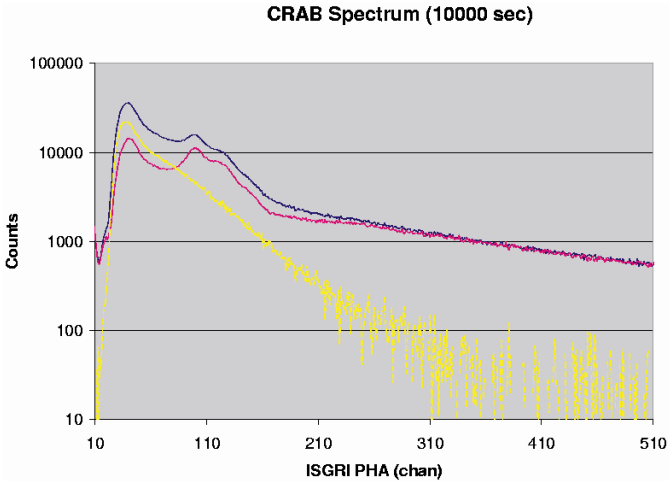

Fig. 17. The Crab count rate spectrum: 10 ks integration time. The three curves show: magenta, background spectrum; blue, On-Source spectrum (i.e., background plus Crab); yellow, Crab only. (Courtesy of A. Segreto).

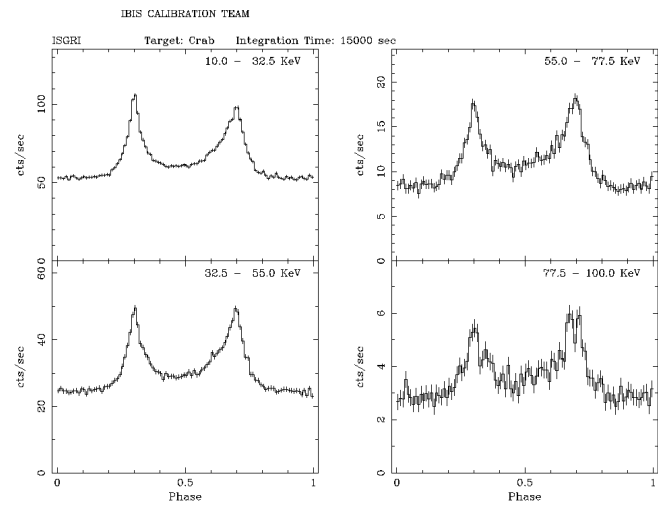

Fig. 18. Crab Pulsar light curve: energy range 14−100 keV (Courtesy of A. Segreto).

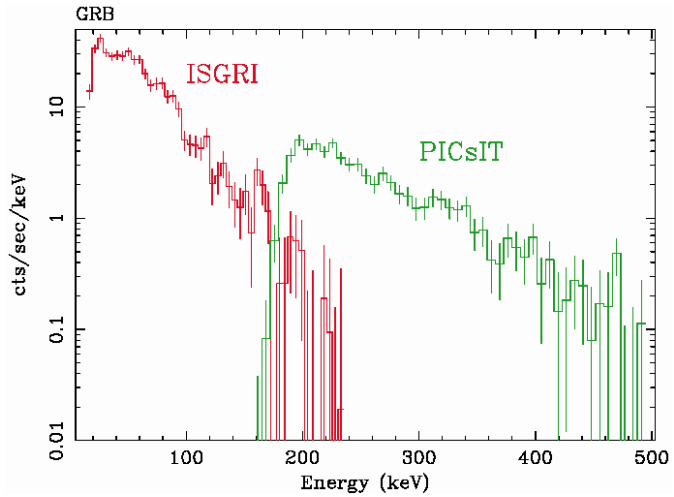

Fig. 19. IBIS detectors counting rate versus energy recorded during the strong GRB 251102. The two detection layers overlap at ~200 KeV. (Courtesy of A. Segreto.)

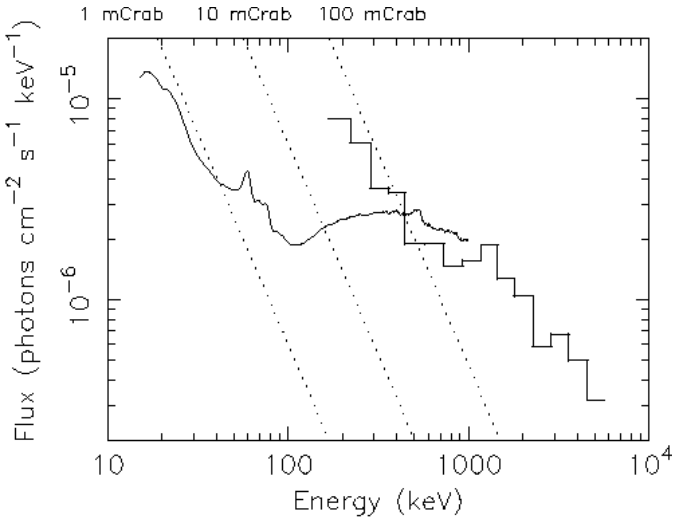

Fig. 20. IBIS continuum sensitivity: 3σ, observing time 10^5 s, $\Delta E = E/2$ single events.

6. IBIS sensitivity

The IBIS continuum sensitivity (3σ, observing time 10^5 s, $\Delta E = E/2$) was recently computed taking into account the measured Background values, in all scientific modes. The IBIS sensitivity, separated in the two ISGRI (left) and PICsIT (right) component is shown in Fig. 20. The values correspond to statistical limit with the observed background, assuming statistical errors only, i.e. systematic errors due to background time and spatial non uniformity etc are not considered. The first two energy bins of the PICsIT curve, in the Spectral Imaging Mode are affected by the "tracks" resulting in a worsening of a factor ~4.0 and ~1.8 for the first and second energy bin, respectively. This effect is fully recovered in photon/photon Mode.

Acknowledgements. The authors wish to emphasize the intellectual and technological contribution of about 300 scientists, engineers and technical people that have made IBIS a reality in space.

We also acknowledge the National Space Agencies and Scientific Institutions that have financed and supported the Co-PIs and Co-Is along the 10 years of the programme development, testing and launch.

The PI acknowledge the Italian Space Agency continuous financial and programmatic support. A special reward to Laben SpA that has lead the building, testing and delivering of this "state of art" gamma ray Imager.

The data reported in the paper are based on observations with INTEGRAL, an ESA project with instruments and science data centre funded by ESA member states (especially the PI countries: Denmark, France, Germany, Italy, Switzerland, Spain), Czech Republic and Poland, and with the participation of Russia and the USA. The Norwegian contribution was funded by Norwegian Research Council (NRC). A special thank to A. Segreto for the outstanding real time IBIS ground support equipment availability and operations. PU is grateful to C. Spalletta for careful preparation and editing of the manuscript.

References

Bazzano, A., Bird, A. J., Capitanio, F., et al. 2003, A&A, 411, L389
Bird, A. J., Bazzano, A., Ferguson, C., et al. 2003a, A&A, 411, L197
Bird, A. J., Barlow, E. J., Bazzano, A., et al. 2003b, A&A, 411, L159
Di Cocco, G., Caroli, E., Celesti, E., et al. 2003, A&A, 411, L189
Goldwurm, A., David, P., Foschini, L., et al. 2003, A&A, 411, L223
Hurley, K. 1978, A&A, 69, 313
Labanti, C., Di Cocco, G., Ferro, G., et al. 2003, A&A, 411, L149
Lebrun, F., Leray, J. P., Lavocat, P., et al. 2003, A&A, 411, L141
Malaguti, G., Bazzano, A., Bird, A. J., et al. 2003, A&A, 411, L173
Natalucci, L., Bird, A. J., Bazzano, A., et al. 2003, A&A, 411, L209
Quadrini, E. M., Bazzano, A., Bird, A. J., et al. 2003, A&A, 411, L153
Segreto, A., Labanti, C., Bazzano, A., et al. 2003, A&A, 411, L215
Stephen, J., Caroli, E., Malizia, A., et al. 2003, A&A, 411, L203
Terrier, R., Lebrun, F., Bazzano, A., et al. 2003, A&A, 411, L167
Ubertini, P., Lebrun, F., Di Cocco, G., et al. 1999, AIP Conf., 510, 684
Ubertini, P. 2003, Proc. of the Symp. The Restless Universe, Amsterdam, 7–8 May, in press
Winkler, C. 2001, in Exploring the gamma-ray Universe, Proc. 4th Integral Workshop, ed. A. Gimenez, V. Reglero, & C. Winkler, ESA SP- 459, 471
Winkler, C., Gehrels, N., Schönfelder, V., et al. 2003, A&A, 411, L349